Robotica (2008) volume 26, pp. 781–790. © 2008 Cambridge University Press
doi:10.1017/S0263574708004372 Printed in the United Kingdom

A bilateral teleoperation controller considering the transition between the free space motion and the constrained motion

Heng Wang†, K. H. Low*† and Michael Yu Wang‡

†*School of Mechanical and Aerospace Engineering, Nanyang Technological University, Singapore 639798*
‡*Department of Mechanical and Automation Engineering, The Chinese University of Hong Kong, Hong Kong, China.*

(Received in Final Form: February 11, 2008. First published online: March 18, 2008)

SUMMARY
A two-channel bilateral controller is proposed for teleoperation systems. The controller takes into account both the free space motion and the constrained motion. Specifically, the force-position (F-P) architecture is applied during the constrained motion, while the position-position (P-P) architecture is applied during the free space motion. Theoretically, perfect transparency can be achieved. In addition, it does not need to switch the control modes of the master and the slave controllers during the transition between the free space motion and the constrained motion. Experiments are conducted to validate the analysis, and to demonstrate the effectiveness of the proposed bilateral controller. The limitations of the proposed controller are also discussed.

KEYWORDS: Teleoperation; Bilateral control; Transparency; Transition of motion.

1. Introduction

A typical teleoperation system consists of five components, which are the human operator, the master device, the slave manipulator, the environment, and the communication channel. The major objective in designing the teleoperation control system is to achieve transparency provided that the system is stable. In a transparent system, both the position and the force at the master and the slave are well matched.

The four-channel architecture developed by Lawrence[1] has been widely used as the tool to analyze the teleoperation system and to design the controller. It has been proven that, in theory, the perfect transparency can be achieved by transmitting both master and slave positions and forces.[1,2] It is claimed that this achievement is due to the use of all four channels of data transmission. Subsequently, Hashtrudi-Zaad and Salcudean[3] showed that the architecture with only three channels can realize perfect transparency by employing local force feedback. Recently, by analyzing the four-channel architecture with local force feedback, Kim *et al.*[4] showed that perfect transparency can be achieved in the position-force (P-F) and force-position (F-P) two-channel architectures. Note that in this paper, the P-F architecture is the system in which the position information is sent from the master to the slave, and the force information is sent from the slave to the master. This result conforms to the observations by Fite *et al.*[5,6] in which the authors addressed the transparency and stability of the P-F two-channel system from a frequency domain loop-shaping perspective. It was shown that the transparency and the stability robustness can be simultaneously improved in a teleoperation system.

In the analysis performed based on the four-channel architecture, the system is idealized as the linear one. However, the master and slave manipulators usually have complex coupled nonlinear dynamics. It is therefore advantageous to apply the well developed single manipulator control schemes to the teleoperation systems, in that these schemes take into account the uncertainties and disturbances. Toward this end, the impedance control technique[7] has been widely applied in designing teleoperation control systems.[8–10] However, the transparency was not discussed in these work. By extending the idea of parallel force/position control for single robot control,[11] Hashtrudi-Zaad and Salcudean[12] proposed a four-channel bilateral parallel force/position controller with perfect transparency achieved. Although the analysis and the experiments were performed for the linear single degree of freedom system, it can be expected that this controller can improve the force and position tracking performance in the presence of system parameter and dynamic uncertainties.

Many tasks include both the unconstrained motion and the constrained motion. Previous works mainly focus on the constrained motion without considering the transition between the unconstrained and the constrained motions. In general, the controllers of the master and the slave have different control modes in free space and in constrained condition. It is desired that the master and the slave both have a single control law for the constrained and unconstrained motions without switch of control modes. The force/moment accommodation (FMA) technique is applied in teleoperation systems[13–15] in which the control mode switch is not required during the transition of motion. However, the transparency is not considered in these work.

In our previous work, a combined impedance/direct control structure was proposed for single manipulator control[16] in which the control mode switch is not required during the transition of motion between the unconstrained and the

* Corresponding author: E-mail: mkhlow@ntu.edu.sg

https://doi.org/10.1017/S0263574708004372 Published online by Cambridge University Press

constrained conditions. In addition, the scheme is more robust to uncertainties and disturbances, if compared with typical impedance control. Considering the transition of motion, a two-channel bilateral controller is proposed in this work by applying the combined impedance/direct control. Perfect transparency can be achieved in theory. In addition, no control mode switch is required during the transition of motion.

In the following, the combined impedance/direct control is first reviewed in Section 2. Next, the master and slave controllers are proposed with the transparency and stability analysis. The problem of transition of motion is then addressed. The experimental results are then presented in Section 5 to verify the analysis. Finally, concluding remarks are drawn.

2. Review of Combined Impedance/Direct Control

The combined impedance/direct controller is formulated based on the torque-based impedance controller. Considering only the translational motion of the end-effector, the equation of motion of a general manipulator can be expressed in Cartesian space as

$$\mathbf{D}_x(\mathbf{q})\ddot{\mathbf{X}} + \mathbf{H}_x(\mathbf{q}, \dot{\mathbf{q}}) = \mathbf{F} - \mathbf{F}_e + \mathbf{F}_{dist} \tag{1}$$

where $\mathbf{X} \in \mathbb{R}^3$ is the robot Cartesian position, $\mathbf{q} \in \mathbb{R}^n$ denotes the joint angles, $\mathbf{D}_x(\mathbf{q}) \in \mathbb{R}^{3\times3}$ is the Cartesian inertia matrix, $\mathbf{H}_x(\mathbf{q}, \dot{\mathbf{q}}) \in \mathbb{R}^3$ includes the terms of Cartesian Coriolis and centrifugal force, and the Cartesian gravitational force, $\mathbf{F}_e \in \mathbb{R}^3$ is the force exerted by the end-effector to the environment, $\mathbf{F}_{dist} \in \mathbb{R}^3$ denotes the external disturbance force acted on the end-effector, and $\mathbf{F} \in \mathbb{R}^3$ is the control input.

Let $\mathbf{X}_r$ represent the reference trajectory, and the positive definite diagonal matrices $\mathbf{M}_t, \mathbf{B}_t, \mathbf{K}_t \in \mathbb{R}^{3\times3}$ denote the target inertia, damping, and stiffness, respectively. By defining the target impedance as

$$\mathbf{M}_t\ddot{\mathbf{E}}_x + \mathbf{B}_t\dot{\mathbf{E}}_x + \mathbf{K}_t\mathbf{E}_x = \mathbf{F}_e \tag{2}$$

where

$$\mathbf{E}_x = \mathbf{X}_r - \mathbf{X}, \tag{3}$$

the typical torque-based impedance control law is then expressed as

$$\mathbf{F} = \hat{\mathbf{D}}_x\mathbf{U} + \hat{\mathbf{H}}_x + \mathbf{F}_e \tag{4}$$

where $\hat{\mathbf{D}}_x$ and $\hat{\mathbf{H}}_x$ are the estimates of $\mathbf{D}_x$ and $\mathbf{H}_x$, respectively, and

$$\mathbf{U} = \ddot{\mathbf{X}}_r + \mathbf{M}_t^{-1}(\mathbf{B}_t\dot{\mathbf{E}}_x + \mathbf{K}_t\mathbf{E}_x - \mathbf{F}_e) \tag{5}$$

By assuming that the environment can be modeled as a linear mass-damper-spring system, $\mathbf{X}_r$ in the constrained condition can be designed as[17]

$$\mathbf{X}_r = \mathbf{X}_{eo} + \mathbf{K}_{eq}^{-1}\mathbf{F}_d \tag{6}$$

where $\mathbf{X}_{eo} \in \mathbb{R}^3$ is the initial environment position without contacting the end-effector, $\mathbf{K}_e \in \mathbb{R}^{3\times3}$ is the diagonal environment stiffness matrix, and $\mathbf{F}_d \in \mathbb{R}^3$ is the desired force, and

$$\mathbf{K}_{eq} = \mathbf{K}_t(\mathbf{K}_e + \mathbf{K}_t)^{-1}\mathbf{K}_e. \tag{7}$$

It has been shown in ref. 18 that with the presence of un-predicable disturbances, the performance of impedance control cannot be guaranteed. Based on the analysis of the closed-loop system equation, the combined impedance/direct controller was proposed as[16]

$$\mathbf{F} = \hat{\mathbf{D}}_x\left(\mathbf{U} + \mathbf{K}_p\mathbf{E}_f + \mathbf{K}_i\int_0^t \mathbf{E}_f\,dt\right) + \hat{\mathbf{H}}_x + \mathbf{F}_e \tag{8}$$

where $\mathbf{K}_p$ and $\mathbf{K}_i \in \mathbb{R}^{3\times3}$ are diagonal matrices, and

$$\mathbf{E}_f = \mathbf{F}_d - \mathbf{F}_e. \tag{9}$$

The combined impedance/direct controller actually combines the advantages of both the impedance control and the direct force control. By properly incorporating a force error based PI-type compensator into the impedance controller, the model uncertainties and the external disturbances are handled directly, which is the advantage of the direct force control. It has been shown in ref. 16 that the combined impedance/direct controller is more robust to model and environmental uncertainties, and has higher disturbance rejection capability. On the other hand, since $\mathbf{E}_f = \mathbf{0}$ holds in free space motion, the controller becomes a pure impedance controller in the unconstrained motion. Therefore, it does not need to switch the control modes when the end-effector transfers between the unconstrained motion and the constrained motion, which is the advantage of the impedance control. In the next two sections, the master and the slave controllers of the teleoperation system are presented by applying the combined impedance/direct control scheme.

3. Bilateral Control Scheme Design in Constrained Motion

The control schemes for single manipulator control usually have position or force command as the single input. Since perfect transparency can be achieved in two-channel control architectures,[4] the well developed single robot control schemes can be applied to design the bilateral controller. By doing this, it is desired to improve the system robustness to the uncanceled nonlinear dynamics and possible external disturbances. In this work, the F-P architecture is employed in the constrained bilateral controller, where the force information is transmitted from the master to the slave and the position information is transmitted from the slave to the master. Specifically, the combined impedance/direct control scheme is applied on the slave, while a position control scheme with local force compensation is employed on the

https://doi.org/10.1017/S0263574708004372 Published online by Cambridge University Press

master. The following section gives details of the controller design.

3.1. Master and slave controller design

Recall the robot dynamic Eq. (1), without considering the external disturbance, the master and slave dynamics are modeled as

$$\mathbf{F}_{mc} = \mathbf{D}_{xm}\ddot{\mathbf{X}}_m + \mathbf{H}_{xm} - \mathbf{F}_h \tag{10}$$

$$\mathbf{F}_{sc} = \mathbf{D}_{xs}\ddot{\mathbf{X}}_s + \mathbf{H}_{xs} + \mathbf{F}_e \tag{11}$$

where $\mathbf{D}_{xm}$ and $\mathbf{D}_{xs}$ respectively represent the master and the slave inertia matrices; $\mathbf{H}_{xm}$ and $\mathbf{H}_{xs}$ respectively denote the master and the slave terms corresponding to $\mathbf{H}_x$ in (1); $\mathbf{X}_m$ and $\mathbf{X}_s$ are respectively the master and the slave positions; $\mathbf{F}_h$ and $\mathbf{F}_e$ are respectively the force exerted on the master by the operator, and the force applied on the environment by the slave; and $\mathbf{F}_{mc}$ and $\mathbf{F}_{sc}$ denote the control inputs of the master and the slave, respectively.

The environment is modeled as a linear time invariant (LTI) mass-damper-spring system, which is expressed in frequency domain as

$$\mathbf{F}_e(s) = (\mathbf{M}_e s^2 + \mathbf{B}_e s + \mathbf{K}_e)(\mathbf{X}_s(s) - \mathbf{X}_{eo}(s)) \tag{12}$$

where $\mathbf{M}_e$, $\mathbf{B}_e$, and $\mathbf{K}_e \in \mathbb{R}^{3\times3}$ are the diagonal matrices representing the environment mass, damping, and stiffness coefficients, respectively. The operator dynamics is also modeled as LTI mass-damper-spring system, which is expressed in frequency domain as

$$\mathbf{F}_h(s) = \mathbf{F}_h^*(s) - \mathbf{Z}_h\mathbf{V}_h(s) \tag{13}$$

where $\mathbf{X}_h = \mathbf{X}_m$ is the human position, $\mathbf{F}_h^*$ is the operator exogenous input force, and $\mathbf{Z}_h$ denotes the operator impedance matrix, which is defined as

$$\mathbf{Z}_h = \mathbf{M}_h s + \mathbf{B}_h + \frac{\mathbf{K}_h}{s} \tag{14}$$

with $\mathbf{M}_h$, $\mathbf{B}_h$, and $\mathbf{K}_h \in \mathbb{R}^{3\times3}$ representing the operator mass, damping, and stiffness matrices, respectively.

In the constrained motion, we have $\mathbf{F}_{ed} = \mathbf{F}_h$, where $\mathbf{F}_{ed}$ denotes the desired force applied on the environment by the slave robot. According to the combined impedance/direct controller represented by (8), the following controller is proposed for the slave

$$\mathbf{F}_{sc} = \mathbf{D}_{xs}\left(\mathbf{U}_s + \mathbf{K}_{ps}\mathbf{E}_{fs} + \mathbf{K}_{is}\int_0^t \mathbf{E}_{fs}\,dt\right) + \mathbf{H}_{xs} + \mathbf{F}_e \tag{15}$$

where

$$\mathbf{E}_{fs} = \mathbf{F}_h - \mathbf{F}_e \tag{16}$$

$$\mathbf{U}_s = \mathbf{M}_{ts}^{-1}(\mathbf{B}_{ts}\dot{\mathbf{E}}_{xs} + \mathbf{K}_{ts}\mathbf{E}_{xs} - \mathbf{F}_e) \tag{17}$$

$$\mathbf{E}_{xs} = \mathbf{X}_{rs} - \mathbf{X}_s \tag{18}$$

$$\mathbf{X}_{rs} = \mathbf{X}_{eo} + \mathbf{K}_e^{-1}(\mathbf{K}_e + \mathbf{K}_{ts})\mathbf{K}_{ts}^{-1}\mathbf{F}_h. \tag{19}$$

The nomenclature is basically the same as that defined in Section 2, with the adding letter *s* in the subscript representing the *slave*. Note that the slave acceleration is not needed to implement the slave controller.

For the master, we have $\mathbf{X}_{md} = \mathbf{X}_s$, where $\mathbf{X}_{md}$ is the desired master position. A position error based controller with local force compensation is employed, which is

$$\mathbf{F}_{mc} = \mathbf{D}_{xm}\Big[\ddot{\mathbf{X}}_s + \mathbf{K}_{vm}\dot{\mathbf{E}}_{ms} + \mathbf{K}_{pm}\mathbf{E}_{ms} + \mathbf{K}_{im}\int_0^t \mathbf{E}_{ms}\,dt\Big] + \mathbf{H}_{xm} - \mathbf{F}_h \tag{20}$$

where

$$\mathbf{E}_{ms} = \mathbf{X}_s - \mathbf{X}_m \tag{21}$$

and the letter m in the subscript represent the *master* and the diagonal matrices $\mathbf{K}_{vm}$, $\mathbf{K}_{pm}$, and $\mathbf{K}_{im}$ are the master control parameters. To implement the master controller (20), the slave acceleration is needed. If acceleration signal is noisy due to the numerical differentiation of the digital encoder readings, the terms with acceleration can be ignored, while the transparency decreases at high frequencies.

By combining (10) and (20), (11) and (15), the closed-loop dynamic equations can be obtained as

$$\ddot{\mathbf{X}}_s - \ddot{\mathbf{X}}_m + \mathbf{K}_{vm}(\dot{\mathbf{X}}_s - \dot{\mathbf{X}}_m) + \mathbf{K}_{pm}(\mathbf{X}_s - \mathbf{X}_m) + \mathbf{K}_{im}\int_0^t (\mathbf{X}_s - \mathbf{X}_m)\,dt = \mathbf{0} \tag{22}$$

for the master, and

$$\begin{aligned}&\big(\mathbf{M}_{ts}^{-1}\mathbf{K}_{ts}\mathbf{K}_{eqs}^{-1} + \mathbf{K}_{ps}\big)(\mathbf{F}_h - \mathbf{F}_e) + \mathbf{K}_{is}\int_0^t (\mathbf{F}_h - \mathbf{F}_e)dt \\ &= \mathbf{M}_{ts}^{-1}\big(\mathbf{M}_{ts} + \mathbf{M}_e - \mathbf{K}_{ts}\mathbf{K}_{eqs}^{-1}\mathbf{M}_e\big)\ddot{\mathbf{X}}_s \\ &\quad + \mathbf{M}_{ts}^{-1}(\mathbf{B}_{ts} + \mathbf{B}_e - \mathbf{K}_{ts}\mathbf{K}_{eqs}^{-1}\mathbf{B}_e)\dot{\mathbf{X}}_s\end{aligned} \tag{23}$$

for the slave.

Taking Laplace transform of (22) and (23), and without loss of generality, the closed-loop dynamics can be expressed in frequency domain for a single degree of freedom as

$$(X_s - X_m)s^2 + k_{vm}(X_s - X_m)s + k_{pm}(X_s - X_m) + k_{im}(X_s - X_m)\frac{1}{s} = 0 \tag{24}$$

for the master, and

$$\begin{aligned}&\left(\frac{k_{ts}}{m_{ts}k_{eqs}} + k_{ps} + \frac{k_{is}}{s}\right)\big(F_h - F_e\big) \\ &= \left(1 + \frac{m_e}{m_{ts}} - \frac{m_e k_{ts}}{m_{ts}k_{eqs}}\right)s^2 X_s \\ &\quad + \left(\frac{b_{ts}}{m_{ts}} + \frac{b_e}{m_{ts}} - \frac{b_e k_{ts}}{m_{ts}k_{eqs}}\right)sX_s\end{aligned} \tag{25}$$

https://doi.org/10.1017/S0263574708004372 Published online by Cambridge University Press

for the slave, where the parameters in small letters are the components of their corresponding matrices in (22) and (23), and X_m, X_s, F_h, and F_e are the Laplace transform of x_m, x_s, f_h, and f_e, respectively.

Assume that the environment initially rests at $x_{eo} = 0$ and f_h^* is constant, then the steady state analysis of (12), (13), (24), and (25) yields

$$\overline{x}_h \equiv \overline{x}_m = \overline{x}_s \equiv \overline{x}_e = \frac{f_h^*}{k_h + k_e} \tag{26}$$

$$\overline{f}_h = \overline{f}_e = \frac{k_e f_h^*}{k_h + k_e} \tag{27}$$

where $\overline{(\cdot)}$ denotes the steady state value of the argument. Equations (26) and (27) show that the master and slave steady state position and force are decided by the operator and environment stiffness coefficients and the operator exogenous force input. It is also easy to verify that $\overline{f}_h/\overline{x}_h = k_e$, i.e., the transparency is fully achieved in steady state. The transparency analysis is further addressed next.

3.2. *Transparency analysis*

The four-channel architecture with local force feedback is shown in Fig. 1 from which the closed-loop dynamic equations of the master and the slave can be obtained as

$$(Z_m + C_m)V_h + C_4 V_e + C_2 F_e - (1 + C_6)F_h = 0 \tag{28}$$

$$(Z_s + C_s)V_e - C_1 V_h - C_3 F_h + (1 + C_5)F_e = 0 \tag{29}$$

Kim *et al.*[4] have derived the transparency condition of the F-P architecture as

$$\begin{cases} C_3 = 1 + C_5 \neq 0 \\ C_4 = -(Z_m + C_m) \neq 0 \\ C_6 = -1 \\ C_s = -Z_s. \end{cases} \tag{30}$$

For the master, by comparing the closed-loop dynamics of the proposed master controller and the four-channel architecture, i.e., (24) and (28), and considering $V_e(s) = V_s(s) = sX_s(s)$ and $V_h(s) = V_m(s) = sX_m(s)$, one obtains

$$\begin{cases} C_4 = -(Z_m + C_m) = -\left(s^2 + k_{vm}s + k_{pm} + \frac{k_{im}}{s}\right) \neq 0 \\ C_2 = 0 \\ C_6 = -1. \end{cases} \tag{31}$$

Similarly, comparing (29) and (25), and considering $V_e(s) = V_s(s) = sX_s(s)$ yields

$$\begin{cases} C_s + Z_s = \frac{1}{m_{ts}}\left(m_{ts} + m_e - \frac{k_{ts}}{k_{eqs}}m_e\right)s \\ \qquad\qquad + \frac{1}{m_{ts}}\left(b_{ts} + b_e - \frac{k_{ts}}{k_{eqs}}b_e\right) \\ C_3 = 1 + C_5 = \frac{k_{ts}}{m_{ts}k_{eqs}} + k_{ps} + \frac{k_{is}}{s} \\ C_1 = 0. \end{cases} \tag{32}$$

By comparing (31) and (32) with the transparency condition of the F-P architecture represented by (30), it can be seen that the perfect transparency can be achieved if $\frac{k_{ts}}{m_{ts}k_{eqs}} + k_{ps} + \frac{k_{is}}{s} \neq 0$, and

$$m_{ts} + m_e - \frac{k_{ts}}{k_{eqs}}m_e = 0 \tag{33}$$

$$b_{ts} + b_e - \frac{k_{ts}}{k_{eqs}}b_e = 0. \tag{34}$$

By substituting $k_{eqs} = k_e k_{ts}/(k_e + k_{ts})$ into (33) and (34), a condition set for perfect transparency can then be derived as

$$\begin{cases} \frac{k_{ts}}{m_{ts}} = \frac{k_e}{m_e}; \quad \frac{k_{ts}}{b_{ts}} = \frac{k_e}{b_e} \\ k_{pm} \neq 0. \end{cases} \tag{35}$$

Therefore, in theory, transparent teleoperation is attainable in the F-P two-channel architecture with the combined impedance/direct controller employed for the slave, and the position error based controller with local force compensation employed for the master, provided that the condition set (35) is satisfied. It can be shown that, if $\mathbf{K}_{im} = \mathbf{0}$, the transparency condition is the same as (35).

By observing the perfect transparency condition (35), it can be found that the force error based compensator at the slave does not contribute to the system transparency. In other words, ideally there is no difference whether the combined impedance/direct controller or the basic impedance controller is employed at the slave in terms of attainable transparency. However, in practice, un modeled dynamics, uncertainties, and external disturbances may exist. The combined impedance/direct control is more robust to these disturbances and generates more accurate force tracking results than the basic impedance control, which has been shown in ref. 16. Similarly, in the discussed bilateral

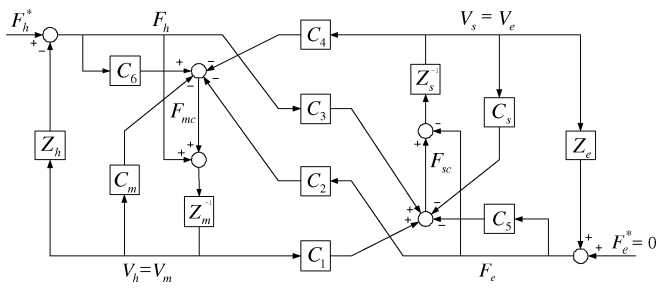


Fig. 1. Four-channel architecture with local force feedback.[3]

https://doi.org/10.1017/S0263574708004372 Published online by Cambridge University Press

control system, the force error based PI-type compensator $k_{ps} + \frac{k_{is}}{s}$ in C_3 can improve the performance by rejecting the disturbances in practical situations.

Another observation is that the environment impedance is required to be known to achieve perfect transparency. In fact, the environment impedance information has the same function as a force or position information channel, and that is why two-channel control architectures can achieve perfect transparency. It will be shown in Section 5 that, for the proposed controller, the system is not transparent when the environment stiffness is estimated with error. The limitation actually applies to all the two-channel bilateral controllers.

3.3. Stability analysis

In this section, we analyze the stability conditions with optimized transparency (i.e., condition set (35) is satisfied) using the recent results by Hashtrudi-Zaad and Salcudean,[3] who have shown that for the transparency-optimized teleoperation systems, the characteristic equation may be written as

$$[C_2(Z_s + C_s) + C_3(Z_m + C_m)](Z_h + Z_e) = 0 \tag{36}$$

which indicates that the system is stable, if the equation

$$C_2(Z_s + C_s) + C_3(Z_m + C_m) = 0 \tag{37}$$

has all roots in the left half-plane. Substituting (3.2) and (32) into (37) and combining (35) yields the characteristic equation of the system, we consider

$$a_4 s^4 + a_3 s^3 + a_2 s^2 + a_1 s + a_0 = 0 \tag{38}$$

where

$$a_0 = k_{im} k_{is} m_e k_{ts} \tag{39}$$

$$a_1 = k_{im} k_{ts} + k_{im} k_{ps} m_e k_{ts} + k_{pm} k_{is} m_e k_{ts} + k_{im} k_e \tag{40}$$

$$a_2 = k_{vm} k_{is} m_e k_{ts} + k_{pm} k_e + k_{pm} k_{ts} + k_{pm} k_{ps} m_e k_{ts} \tag{41}$$

$$a_3 = k_{vm} k_{ts} + k_{vm} k_{ps} m_e k_{ts} + k_{is} m_e k_{ts} + k_{vm} k_e \tag{42}$$

$$a_4 = k_e + k_{ts} + k_{ps} m_e k_{ts}. \tag{43}$$

The stability condition can then be derived according to Hurwitz criteria. A problem is that the stability condition of the fourth-order system is more or less complex. The selected parameter values should be verified to satisfy the stability condition, possibly with the aid of computer computation.

Let us consider the situation that the master controller has no integral term of the position error, i.e., $\mathbf{K}_{im} = \mathbf{0}$. It is easy to verify that the transparency condition (35) maintains the same as the situation with integral term, while the order of characteristic Eq. (38) reduces by one. As a result, according to Hurwitz criteria, the asymptotic stability of the system can be achieved, if the control parameters satisfy the following conditions: $k_e + k_{ts} + k_{ps} m_e k_{ts} > 0$, $k_{vm} k_{ts} + k_{vm} k_{ps} m_e k_{ts} + k_{is} m_e k_{ts} + k_{vm} k_e > 0$, $k_{pm} k_{is} m_e k_{ts} > 0$, and

$$\begin{aligned}(k_{vm} k_{ts} + k_{vm} k_{ps} m_e k_{ts} + k_{is} m_e k_{ts} + k_{vm} k_e)(k_{pm} k_e \\ + k_{pm} k_{ts} + k_{pm} k_{ps} m_e k_{ts} + k_{vm} k_{is} m_e k_{ts}) \\ > \left(k_e + k_{ts} + k_{ps} m_e k_{ts}\right) k_{pm} k_{is} m_e k_{ts}\end{aligned} \tag{44}$$

which can be simplified to

$$\begin{aligned}&2k_{vm} k_{ts} k_{pm} k_e + k_{vm} {k_{ts}}^2 k_{pm} + 2k_{vm} {k_{ts}}^2 k_{pm} k_{ps} m_e \\ &+ {k_{vm}}^2 {k_{ts}}^2 k_{is} m_e + 2k_{vm} k_{ps} m_e k_{ts} k_{pm} k_e \\ &+ k_{vm} {k_{ps}}^2 {m_e}^2 {k_{ts}}^2 k_{pm} + {k_{vm}}^2 k_{ps} {m_e}^2 {k_{ts}}^2 k_{is} \\ &+ {k_{is}}^2 {m_e}^2 {k_{ts}}^2 k_{vm} + k_{vm} {k_e}^2 k_{pm} + {k_{vm}}^2 k_e k_{is} m_e k_{ts} > 0.\end{aligned} \tag{45}$$

Obviously, the system is stable for all positive control parameters. The above analysis shows that, in theory, the bilateral controller without the integral term of the position error at the master has the same transparency condition as that with the integral term, and has a looser stability condition. However, due to the non-ideal condition in practice, a noticeable position tracking error can be observed, if the controller has no integral term at the master. With the addition of the integral term, the performance can be improved, which will be shown by the experimental results in Section 5.

4. Considering Transition of Motion

In the unconstrained motion, the slave robot moves in free space, and $\mathbf{Z}_e = \mathbf{0}$. Therefore, the system is transparent if the operator does not feel the force, and the slave accurately follows the motion of the master. Without the interaction between the slave and the environment, the kinematic correspondence between the master and the slave becomes the primary concern. This situation is simpler than the constrained motion. Intuitively, the position information, rather than the force information, should be transmitted between the master and the slave. As a result, a P-P architecture is suggested in this work for unconstrained motion teleoperation. In addition, it is suggested that the force exerted by the operator to the master is compensated for, such that the feeling of force of the operator in free space is minimized. In this case, the master controller considering both constrained and unconstrained motions can be expressed as

$$\begin{aligned}\mathbf{F}_{mc} = \mathbf{D}_{xm}\Big[&\ddot{\mathbf{X}}_s + \mathbf{K}_{vm}\dot{\mathbf{E}}_{ms} + \mathbf{K}_{pm}\mathbf{E}_{ms} \\ &+ \mathbf{K}_{im}\int_0^t \mathbf{E}_{ms}\,dt\Big] + \mathbf{H}_{xm} - \mathrm{sgn}(\mathbf{F}_e)\mathbf{F}_h,\end{aligned} \tag{46}$$

where in this work the function sgn(·) is defined as

$$\mathrm{sgn}(x) = \begin{cases} 1 & x \neq 0 \\ -1 & x = 0. \end{cases} \tag{47}$$

The slave controller maintains the same as in the constrained motion, since the combined impedance/direct control structure does not require to switch the control

https://doi.org/10.1017/S0263574708004372 Published online by Cambridge University Press

modes during the transition of motion. Specifically, the reference trajectory for the slave is simply set as the master position, i.e., $\mathbf{X}_r = \mathbf{X}_h$, and $\mathbf{F}_h = \mathbf{0}$. Since $\mathbf{F}_e = \mathbf{0}$ in the free space motion, the slave controller is basically the impedance controller. Complete transparency is generally not attainable in the P-P architecture.[4] However, in the extreme situation with $\mathbf{Z}_e = \mathbf{0}$, according to Ni and Wang's result[19] on P-P architecture, we can choose high gains for the slave controller, and low gains for the master controller, such that the transmitted impedance $\mathbf{Z}_t \to \mathbf{0}$. As a result, the extreme condition for the master parameters $\mathbf{K}_{vm} = \mathbf{K}_{pm} = \mathbf{K}_{im} = \mathbf{0}$ is set for the unconstrained motion. Therefore, the same controllers for both the master and the slave as in the constrained motion are used in the unconstrained motion.

The transition of motion between the unconstrained and the constrained conditions is common during most manipulation tasks. The proposed bilateral controller requires no control mode switch of both the master and the slave controllers during the transition of motion. Once the designed controllers are implemented, they can work in both the constrained and unconstrained conditions. The only difference between the constrained and unconstrained conditions is that different communication channels are used. The values of the control parameters $\mathbf{K}_{ts}$, $\mathbf{K}_{pm}$, $\mathbf{K}_{vm}$ and $\mathbf{K}_{im}$ need to be switched when the transition of motion takes place, in order to achieve the perfect transparency. The bilateral controller considering both the constrained and unconstrained motions is thus designed, and the block diagram is shown in Fig. 2.

5. Experiments

In this section, experiments are conducted on a system with two identical single degree of freedom slider-crank mechanisms to validate the effectiveness of the proposed bilateral controller.

5.1. Experimental platform

Figure 3 shows the photograph of the constructed platform. Both the master and the slave are driven by the Emoteq^{TM} direct drive brushless DC motors (QB03400) with the continuous torque up to 0.81 Nm. The encoders with 2000 pulses per revolution are mounted at the end of the motor shafts to measure the angular position. The AMC^{TM} servo amplifiers (B15A) are used to output current commands to the motors. Two simple Honeywell^{TM} one-axis force sensor (FSG15N1A) are attached on the master and the slave, respectively, which are connected to an amplifier circuit to measure the interaction force. The Sensoray^{TM} I/O board

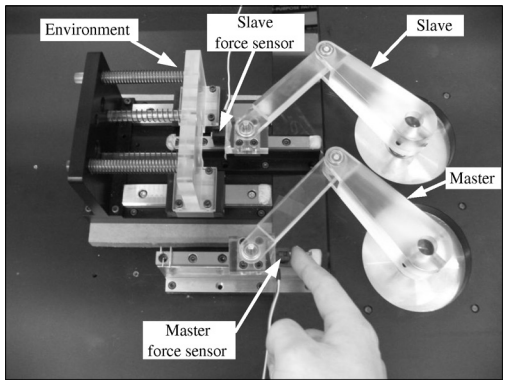


Fig. 3. Teleoperation experimental platform.

(Model 626) is used to read the sensor readings and to output commands to the motors through the amplifiers.

The xPC Target toolbox of Matlab^{TM} is used to implement the control system with the sampling frequency at 1 kHz. In this environment, the Simulink is used to program the control algorithms. The Real Time Workshop and C/C++ compiler then convert the Simulink blocks into C code and build a target application, which is downloaded to the target PC and executed in real-time. Detailed software and hardware implementation can be found in ref. 20.

The slider crank mechanism with the coordinate system of the master and slave is shown in Fig. 4. Without considering the Coulomb and viscous frictions, the dynamic equation can be obtained as

$$d(q)\ddot{q} + c(q)\dot{q} = \tau \tag{48}$$

where the parameters are estimated to be $d(q) = \left(7.10\cos^2 q + 2.58\right) \times 10^{-4}$ kgm^2, and $c(q) = 3.55 \times 10^{-4}\dot{q}\sin(2q)$ kgm^2/s. Note that there are errors between the estimations and the real values. The environment adopts a mass-damper-spring system, which consists of a moving plate mounted on two sliders, and several spring components. The values of the impedance parameters are $m_e = 0.14$ kg, $k_e = 400$ N/m, and b_e is small and unknown.

As addressed, the parameters of the dynamic equation are not known precisely and have uncertainties. One of the objectives of the experiments is to show the robustness of the proposed bilateral controller to the robot dynamics uncertainties. The acceleration term is dropped from the master controller in the experiments. For all the following experiments, $k_{ps} = 90$, $k_{is} = 80$, $m_{ts} = 1$, and $b_{ts} = 10$. Note that if not specified, all the parameters and variables

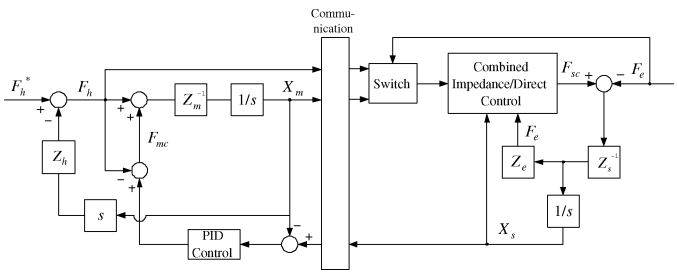


Fig. 2. Block diagram of the proposed bilateral control scheme.

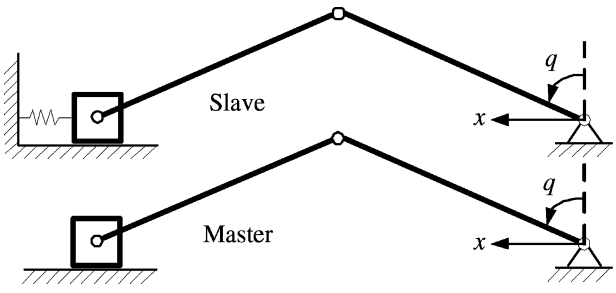


Fig. 4. Slider crank mechanism used in the experiments.

https://doi.org/10.1017/S0263574708004372 Published online by Cambridge University Press

Table 1. MAE and RMSE errors.

		Fig. 1	Fig. 2	Fig. 3	Fig. 4	Fig. 5
Position (mm)	MAE	0.6517	0.5013	0.6420	0.5089	0.4068
	RSME	1.0492	0.6645	0.8055	0.6856	0.5491
Force (N)	MAE	0.0712	0.0712	0.1175	0.4097	0.0600
	RSME	0.0965	0.0965	0.1457	0.5221	0.0820

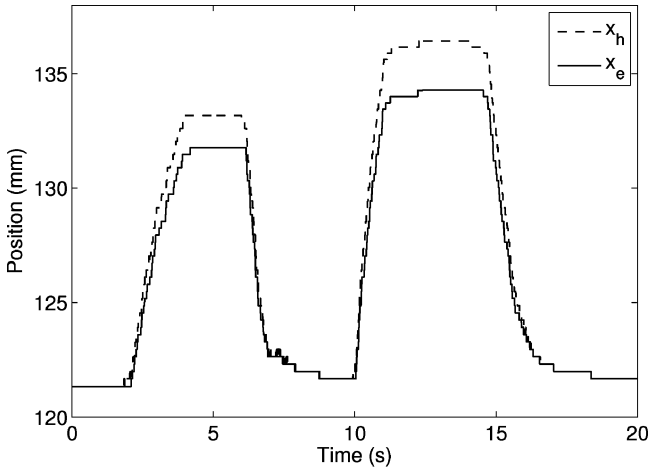
are in SI units, which are omitted for simplicity. During the constrained motion, the parameters of the master controller are set as $k_{pm} = 1.8 \times 10^4$, $k_{vm} = 10$, and $k_{im} = 10^4$. While during the unconstrained motion, $k_{pm} = k_{vm} = k_{im} = 0$.

5.2. *Results of constrained motion*

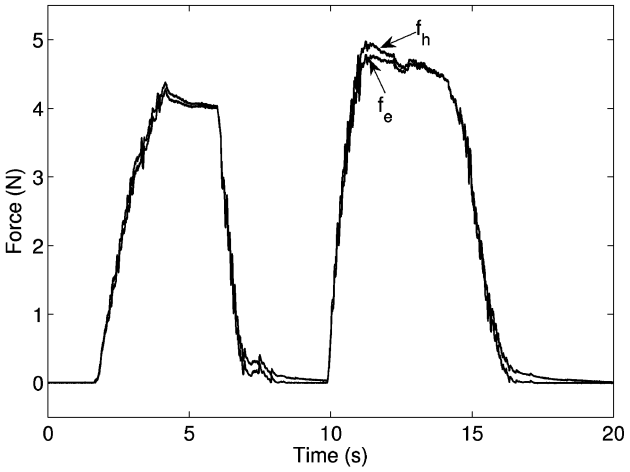
The system performance in the constrained motion is first studied. Before the experiments, the slider of the slave locates at the initial position of the environment $x_{eo} = 122.32$ mm, and the master locates correspondingly. During the experiments, the human operator pushes the master slider along the x-axis direction and then releases gradually. Four sets of experiments are performed. The Mean Absolute Error (MAE) and the Root Mean Squared Error (RMSE) are used to quantitatively evaluate the degree of transparency. Table I summarizes the MAE and RMSE errors of each of the following experimental results for comparison.

Firstly, the controller without the integral term of the position error at the master is implemented. According to the perfect transparency condition (35), the slave target stiffness is set as $k_{ts} = 3000$, such that the system is regarded to be quasi transparent. The results are shown in Fig. 5. The force profiles of the master and the slave (see Fig. 5(b)) show that the interaction force f_e can follow the command f_h with high accuracy. However, a relatively large position error between the master and the slave exists, when the operator pushes the master slider and keeps it at a constant position. The position errors are calculated as MAE = 0.6517 mm and RMSE = 1.0492 mm, while the force errors are MAE = 0.0712 N and RMSE = 0.0965 N. The results reveal that, in practice, it is hard to construct perfect transparent systems, if the controller has no integral term of the position error at the master.

Secondly, the integral term of the position error is included in the master controller, and the results are shown in Fig. 6. The force profiles show a similar tracking result, and the errors are MAE = 0.0712 N and RMSE = 0.0965 N. If compared to the results without the integral term at the master, the position errors are reduced greatly, which are MAE = 0.5013 mm and RMSE = 0.6654 mm. It can be observed that the transient position error still exists, especially during the restoring stage of the environment. This phenomena can be explained as follows. At the stage of pushing, the term $(x_s - x_m)$ is negative, and thus the integral term builds up negative control actions of the master continuously. When the operator releases the master slider gradually, the resultant negative control actions by the integral term will drive the master to move faster than the slave. Another possible reason is that the Coulomb and viscous frictions may dominate the environment dynamics at the restoring stage, which slowers the restoring of the



(a) Position



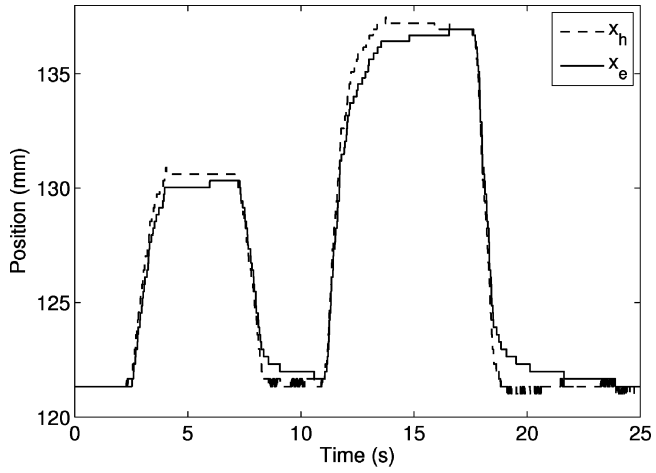
(b) Force

Fig. 5. Results of the quasi transparent system without integral term of position error at the master (k_e and m_e are known, and b_e is unknown).

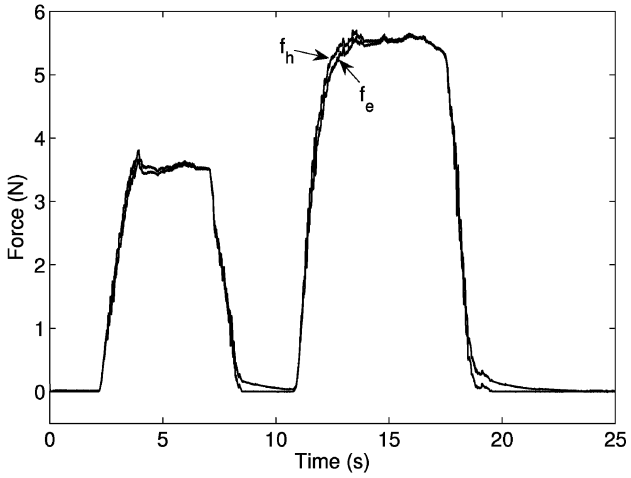
environment. The transient error decreases gradually to zero at the steady state. Another observation is that the integral term introduces a small oscillation into the master position, the amplitude of which is about one encoder count. Note that in the experimental platform, the motors are driven directly without gear-head connected. Overall, the transparency of the system is increased by incorporating the integral term of the position error into the master controller.

Next, the slave target stiffness is set as $k_{ts} = 1.8 \times 10^4$, and therefore the system is nontransparent since the condition set (35) is not satisfied. The results are shown in Fig. 7. If compared to the results shown in Fig. 6, the position errors increase to MAE = 0.6420 mm and RMSE = 0.8055 mm, and the force errors increase to MAE = 0.1175 N and RMSE = 0.1457 N. The results in the first place validate the effectiveness of the transparency condition set (35). On the other hand, the increases of the position and force errors are acceptable in some applications when k_{ts} is increased from 3000 to 1.8×10^4. In other words, the sensitivity of the performance to k_{ts} is low. In this case, the value of k_{ts} can be

https://doi.org/10.1017/S0263574708004372 Published online by Cambridge University Press

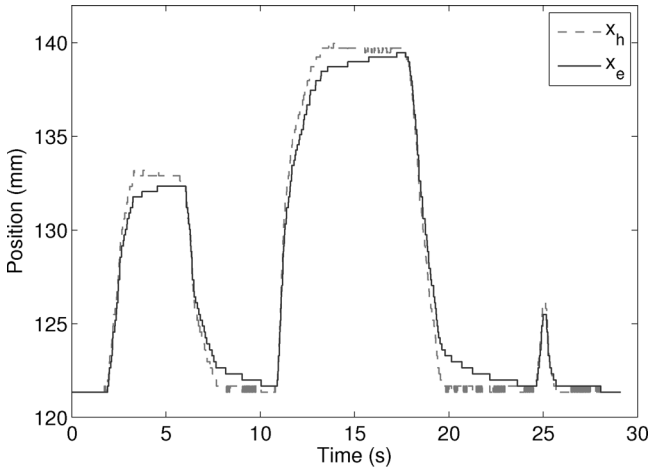


(a) Position

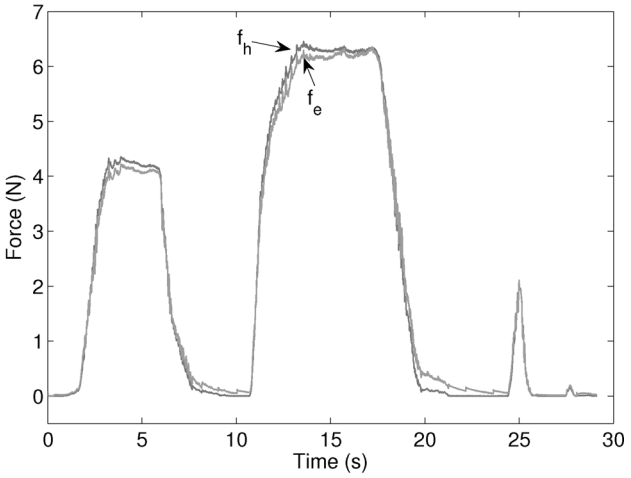


(b) Force

Fig. 6. Results of the quasi transparent system with integral term of position error at the master (k_e and m_e are known, and b_e is unknown).



(a) Position



(b) Force

Fig. 7. Results of nontransparent system with integral term of position error at the master (k_e and m_e are known, and b_e is unknown).

kept unchanged during the transition between the constrained and the unconstrained motions.

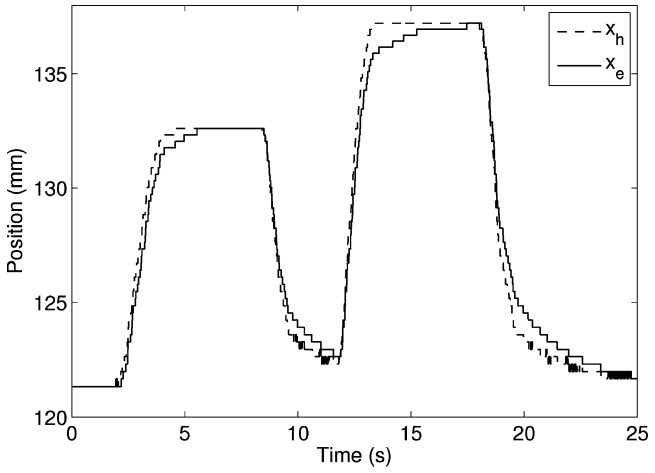
Finally, it is assumed that the environment stiffness is unknown and estimated to be $\hat{k}_e = 2500$. The slave target stiffness is thus designed to be $k_{ts} = 1.8 \times 10^4$, in order to achieve perfect transparency. Figure 8 shows the results. The position errors are small, which are MAE = 0.5089 mm and RMSE = 0.6856 mm. However, the force tracking performance deteriorates drastically, and the errors are MAE = 0.4097 N and RMSE = 0.5221 N. The results comply with the analysis in Section 3.2 that for the two-channel control architectures, the information of the environment impedance is required to be known to achieve perfect transparency.

5.3. *Results of transition of motion*

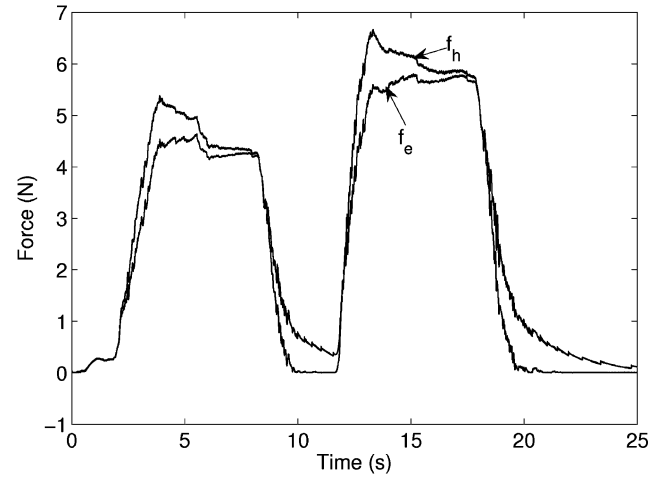
In the experiment of the transition of motion, the slave slider initially locates at $x = 113.10$ mm. So does the master slider. During the experiment, the operator pushes the master slider along the x-axis direction. When the slave slider contacts the environment at $x = 122.32$ mm, the free space motion transits to the constrained motion. Afterwards, the operator repeats to push and then release the master several times, followed by the transition from the constrained motion to the free space motion.

The slave target stiffness is set as $k_{ts} = 1.8 \times 10^4$. Therefore, during the transition of motion, it does not need to switch the control modes and the values of the control parameters of the slave controller. The master controller is also kept un-changed, while the values of the control parameters should be switched from $k_{pm} = k_{vm} = k_{im} = 0$ to $k_{pm} = 1.8 \times 10^4$, $k_{vm} = 10$, and $k_{im} = 10^4$ when the motion transits from the free space to the constrained condition, and vice versa. As shown in Fig. 9, the motion transits smoothly with high transparency in both constrained and unconstrained conditions. The position errors are MAE = 0.4068 mm and RMSE = 0.5491 mm, and the force errors are MAE = 0.0600 N and RMSE = 0.0820 N. In addition, the kinematic correspondence is maintained when the motion transits from the contact condition to the free space, which is important for repetitive and consecutive manipulations.

https://doi.org/10.1017/S0263574708004372 Published online by Cambridge University Press

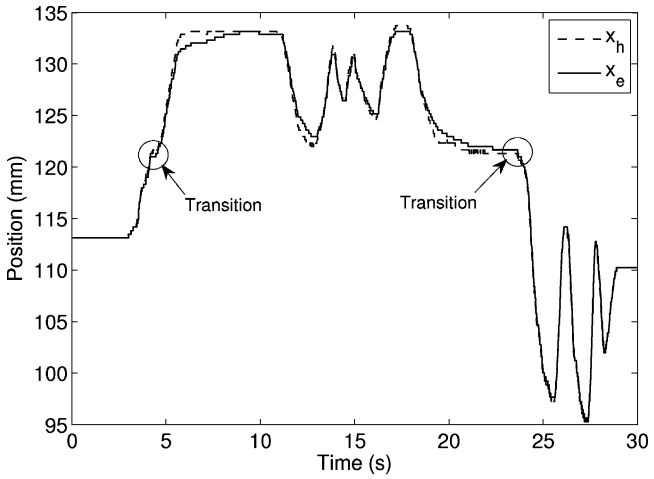


(a) Position

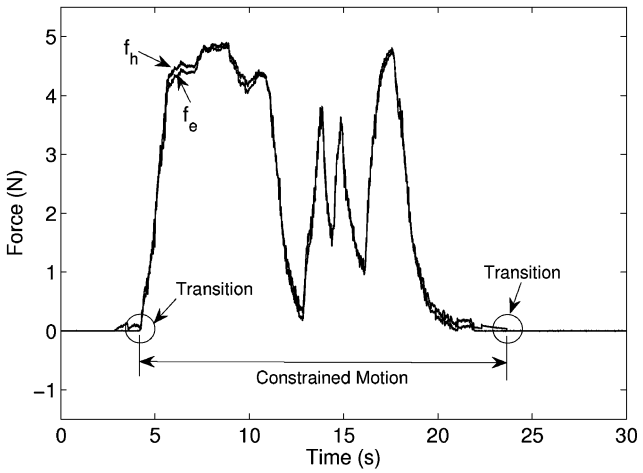


(b) Force

Fig. 8. Results in the case that the environment stiffness is estimated with error (m_e is known, and k_e and b_e are unknown. k_e is estimated as $\hat{k}_e = 2500\,\mathrm{N/m}$).



(a) Position



(b) Force

Fig. 9. Results of a typical operation including transition between the free space motion and the constrained motion (k_e and m_e are known, and b_e is unknown).

6. Concluding Remarks

A two-channel bilateral controller is proposed for teleoperation systems in the present work. The control architecture is constructed by considering both the free space motion and the constrained motion. Specifically, the F-P architecture is applied in the constrained motion, while the P-P architecture is applied in the free space motion. Experimental results validate the analysis, and demonstrate the effectiveness of the proposed bilateral control scheme.

The developed bilateral control scheme has the following features. Firstly, perfect transparency can be achieved in the two-channel control architecture. Secondly, due to the disturbance rejection capability of the combined impedance/direct control, the robot-environment interaction force $\mathbf{F}_e$ can be controlled with high accuracy with the presence of robot dynamic uncertainties and external disturbances. Thirdly, it does not need to switch the control modes of the master and the slave controllers during the transition of motion. Once the designed controllers are implemented they can work in both the constrained and unconstrained conditions. The only difference between the constrained and the unconstrained conditions is that different communication channels are used.

A limitation of the proposed controller is that the environment impedance needs to be known to achieve high degree of transparency. Actually, such a limitation applies to all the two-channel architectures of the teleoperation controllers. In the case that the environment dynamics is unknown, at least three-channel architecture is necessary. Our future work is to expand the presented idea to three-channel or four-channel architectures, such that the system is transparent, and can transit smoothly between the constrained and the unconstrained conditions without knowing the environment impedance. Since there is time delay present in some situations, another future work is to study the influence of time delay for the proposed controller.

References

1. D. A. Lawrence, "Stability and transparency in bilateral teleoperation," *IEEE Trans. Robot. Autom.* **9**(5), 624–637 (1993).

https://doi.org/10.1017/S0263574708004372 Published online by Cambridge University Press

2. Y. Yokokohji and T. Yoshikawa, "Bilateral control of master-slave manipulators for ideal kinematic coupling-formulation and experiment," *IEEE Trans. Robot. Autom.* **10**(5), 605–620 (1994).
3. K. Hashtrudi-Zaad and S. E. Salcudean, "Transparency in time-delayed systems and the effect of local force feedback for transparent teleoperation," *IEEE Trans. Robot. Autom.* **18**(1), 108–114 (2002).
4. J. Kim, P. H. Chang and H.-S. Park, "Transparent Teleoperation using Two-channel Control Architectures," *Proceedings of the IEEE International Conference on Intelligent Robots and Systems (IROS'05)*, Edmonton, Alberta, Canada (Aug. 2005), pp. 2824–2831.
5. K. B. Fite, L. Shao and M. Goldfarb, "Loop shaping for transparency and stability robustness in bilateral telemanipulation," *IEEE Trans. Robot. Autom.* **20**(3), 620–624 (2004).
6. K. B. Fite, J. E. Speich and M. Goldfarb, "Transparency and stability robustness in two-channel bilateral telemanipulation," *J. dyn. Sys. Meas. Control* **123**(3), 400–407 (2001).
7. N. Hogan, "Impedance control: An approach to manipulation. Parts I, II and III," *ASME J. Dyn. Syst. Meas. Control*, **107**(1), 1–24 (1985).
8. H. C. Cho and J. H. Park, "Stable bilateral teleoperation under a time delay using a robust impedance control," *Mechatronics*, **15**(5), 611–625 (2005).
9. W. B. Griffin, W. R. Provancher and M. R. Cutkosky, "Feedback strategies for telemanipulation with shared control of object handling forces," *Presence*, **14**(6), 720–731 (2005).
10. A. Peer, B. Stanczyk, and M. Buss, "Haptic Telemanipulation with Dissimilar Kinematics," *Proceedings of the IEEE International Conference on Intelligent Robots and Systems (IROS'05)*, Edmonton, Alberta, Canada (Aug. 2005), pp. 2483–2488.
11. S. Chiaverini and L. Sciavicco, "The parallel approach to force/position control of robotic manipulators," *IEEE Trans. Robot. Automation*, **9**(4), 361–373 (1993).
12. K. Hashtrudi-Zaad and S. E. Salcudean, "Bilateral parallel force/position teleoperation control," *J. Robot. Syst.* **19**(4), 155–167 (2002).
13. F. Aghili, E. Dupuis, E. Martin and J.-C. Piedboeuf, "Force/moment Accommodation Control for Tele-operated Manipulators performing contact tasks in stiff environment," *Proceedings of the IEEE International Conference on Intelligient Robots and Systems (IROS'01)*, Maui, Hawaii, USA (Oct.–Nov. 2001), pp. 2227–2233.
14. R. L. Williams II, J. M. Henry, and M. A. Murphy, "Free and Constrained Motion Teleoperation via Naturally-Transitioning Rate-to-Force Control," *Proceedings of the IEEE International Conference on Robotics and Automation (ICRA'99)*, Detroit, Michigan (May 1999), pp. 225–230.
15. R. L. Williams II, J. M. Henry and D. W. Repperger, "Evaluation of rate-based, force-reflecting teleoperation in free motion and contact," *Presence*, **9**(1), 25–36 (2000).
16. H. Wang, K. H. Low and M. Y. Wang, "Combined Impedance/direct Control of Robot Manipualtors," *Proceedings of the IEEE International Conference on Intelligient Robots and Systems (IROS'06)*, Beijing, China (Oct. 2006).
17. S. Jung, T. C. Hsia and R. G. Bonitz, "Force tracking impedance control for robot manipulators with an unknown environment: Theory, simulation, and experiment," *Int. J. Robot. Res.* **20**(9), 765–774 (2001).
18. H. Wang, K. H. Low, and M. Y. Wang, "On the Position/force Control of Robotic Manipulators with Model Uncertainty and Random Disturbances," *Proceedings of the IEEE International Conference on Robotics and Mechatronics (RAM'06)*, Bangkok, Thailand (June 2006), pp. 134–139.
19. L. Ni and W. L. Wang, "A gain-switching control scheme for position-error-based bilateral teleoperation system: Contact stability analysis and controller design," *Int. J. Robot. Res.* **23**(3), 255–274 (2004).
20. K. H. Low, H. Wang, K. M. Liew and Y. Cai, "Modeling and motion control of robotic hand for telemanipulation application," *Int. J. Softw. Eng. Knowl. Eng.* **15**(2), 147–152 (2005).

https://doi.org/10.1017/S0263574708004372 Published online by Cambridge University Press